Chapter 4

Fabrication of Low Cost Functionalized Poly (vinylidene fluoride) Nanohybrid Membrane for Superior Fuel Cell

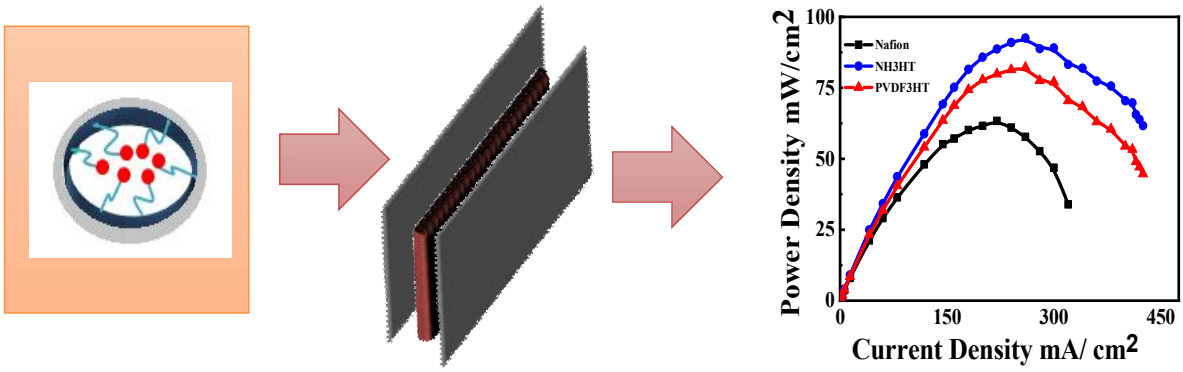

4.1 Introduction:

Power generation (energy demand) from renewable resources is the need of hour in the 21st century to save our environment, fossil fuel, which is exhausting very fast leading to the increase of portable power source demand [116][160]. To fulfill the energy requirements in portable, stationary field there is a need to promote the research in portable energy generating technology such as solar cell, thermal energy, wind energy and fuel cell technology [119], [125], [161], [162]. The major drawbacks of all the above portable power sources are bigger in size and high cost. Now, more efforts have been dedicated to reduce the cost and size of all these commercial portable stationary power sources. Fuel cell technology is one of the promising technology in terms of low cost and small in size for stationary power sources [49]. In fuel cell technology, the electrolyte is a key factor and based on the electrolyte, different type of fuel cell are developed like solid oxide fuel cell [85], molten carbonate fuel cell [163], phosphoric acid fuel cell [164], alkaline fuel cell [165] etc. Amongst them, polymer electrolyte membrane (PEM) or proton exchange membrane gets tremendous attentions in fuel cell and conversion of chemical energy to electrical energy [166], [167]. Polymer based electrolyte membrane is a thin plastic membrane which is used in fuel cell technology electrolyte cum electron separator [133]. The proton exchange capabilities of the membrane is commonly developed through functionalization of polymer chain by different monomers or ionic species like phosphate, sulphate and chloride to transport the ions from one side of the electrode to other side which facilitates the overall chemical reaction and thereby separate electrons [168],[97]. Several methods have been used in literature to introduce different ionomers in polymer chain and, hence, insertion of reactive sites in long chain molecule. Different methods used

to introduce reactive sites in polymer are sol–gel method, phase inversion technique, electron, γ- irradiation and swift heavy ions (SHI) etc. [53] Amongst them, high energy swift heavy ions is one of the most promising particle radiation techniques [53], where SHI is exposed to the polymer film at vacuum followed by loosing most of its energy during passage through thin film [106], [169], [170]. The energy loss occurs either through atomic collision or electronic excitation when interact with macromolecules [98]. However, the path of latent track is predominantly amorphous which can be removed by selective chemical etching to create through nanochannels across the thickness of polymer film. Different size and shape of nanochannels are formed depending upon the factors such as linear energy transfer (LET), size of ions, mass of ions and etching conditions. [5] After the SHI irradiation followed by selective chemical etching, the free radical active sites are exposed in polymer membrane which has potential to initiate the polymerization reaction within the nanochannels when allowed to react with the monomer to form graft copolymer [22-24]. A good proton exchange membrane (PEM) should have the following requirements; (1) high proton conductivity, (2) low fuel crossover, (3) sufficient water uptakes and adequate swelling, and (4) good thermal and mechanical stability both under dry and wet condition along with low cost and long term durability [24-26]. Quest for better membrane is continued to improve the fuel cell technology. Ionomer Nafion117 is one of the most common membrane with good proton conductivity ($\sigma \geq 10^{-2}$ S.cm^{-1}) at low temperature, developed by DuPont Inc. [174]. The disadvantages of this commercially available membrane are high fuel crossover leading to lower cell efficiency, potential and higher temperature instability (0-80 ^{o}C), which limits its use as membrane [175]. In view of the fact that the membrane properties, difficulty in processing and cost of fuel cell systems

are closely related, there is an apparent need for optimized or conceptually new type of membrane. Functionalized poly(ethylene-co-tetrafluoroethylene) (ETFE) has been reported having open circuit voltage upto 0.9 V [176]. Sulfonated poly(arylene ether)s blend with polypyrole (s-PEEK/ppy) is reported in literature as proton exchange membrane with proton conductivity of 6.2×10^{-2} $S.cm^{-1}$, methanol permeability of $2.33\times10^{-7}cm^2.s^{-1}$ and selectivity parameter 0.11×10^5 $Scm^{-3}.s$ [177]. Poly(sulfone) and sulphonated poly(imide)s [178] have shown excellent chemical and thermal stability in fuel cell applications, but their weaker aryl sulphonic acid groups cause lower proton conductivity [23], [19], [168]. Sulphonation of PVDF composite exhibit proton conductivity in the order of 5.0×10^{-3} S cm^{-1} [98] and also fulfill the basic requirements of the proton exchange membrane in fuel cell technology.

Fluoropolymer such as poly(vinylidene difluoride) (PVDF) and its copolymers exhibit properties such as high mechanical and thermal stability, thermoplastic, nonreactive, electrically insulating, durable, biocompatible along well regulated porosity make them suitable for proton exchange membrane [179], [180]. PVDF and its copolymers exist in five different crystalline phases like non polar α, polar β, γ, δ and ε depending on crystallization condition in presence of different dimensional filler. All trans conformation (*TTTT*) (all hydrogen and fluorine are opposite sides of each other in polymer back bone) of polymer exhibits in orthorhombic piezoelectric β phase [152]. Therefore, nucleation of β phase in PVDF is crucial to generate piezoelectric and ferroelectric properties for smart membrane [181]. In order to overcome these shortcomings, focus is given to design low cost ions exchange membrane for fuel cell using accelerator. In this work, nanochannel is fabricated in polymer thin film by irradiation of high energy swift heavy ions followed by

selective etching and subsequent chemical grafting appropriate for proton conduction. The efficiency of fuel cell is examined using these membranes and found its suitability for real applications in fuel cell technology.

4.2 Experimental

4.2.1 Materials: A commercially available SOLEF 6008 granules of poly(vinylidene fluoride) (PVDF) was kindly supplied by Ausimont, Italy for this study. Cloisite 30B [bis(hydroxyethyl) methyl tallow ammonium ion exchanged montmorillonite], Southern clay, U.S., CEC 110 meq/100g was used (Tallow is a mixture of C_{16} &C_{18} long chain alkenes) as nanofiller. Potassium permanganate ($KMnO_4$), LOBA Chemie and sodium hydroxide (NaOH) Himedia chemicals were used as etchant. Potassium meta-bisulphate ($K_2S_2O_5$, LOBA Chemie) was used for the washing purpose. The monomer 3-hexylthiophene (3HT, Sigma-Aldrich, 99+%), chloroform ($CHCl_3$) and methanol (CH_3OH) LOBA Chemie were used for grafting purpose. Chlorosulphonic acid (HSO_3Cl, LOBA Chemical) was used for sulphonation on graft copolymers and preparation of the nanohybrid details process is given in **chapter 2**.

4.2.2 Functionalization of the membrane:

Around 50 μm thin films of *PVDF* and its nanohybrid (*NH*) were irradiated by using 120 MeV Ag^+ ions in a vacuum of 5 $\times 10^{-6}$ mbar at the Inter University Accelerator Center, New Delhi, India. The ion fluence (number of ions per unit area) used was 5×10^7 ions/cm^2 to secure the effect of fluence on membrane properties. For the fuel cell electrolyte membrane fluence 5×10^7 scattered ions from a thin gold foil (250 μg/cm^2) in GPSC chamber (general purpose scattering chamber) was used for fuel cell membrane

measurement of size 4×4 cm^2. The irradiated pristine *PVDF* and its nanohybrid (NH) films were chemically etched using potassium permanganate solution (0.25 mol /*L*) in a highly alkaline medium (9 mol/*L*) at 65 ^oC for 4 h. The etched brownish precipitate of MnO_2 films were quickly immersed in a $K_2S_2O_5$ saturated solution for 15 min followed by washing in distilled water. The residual water at the surface was enwrapped with a filter paper and was dried at 65 ^oC for 24 h in a vacuum oven under reduced pressure. The porous etched films were immersed in the monomer solution (0.5 ml distilled non-ionized form of 3-hexylthiophene (*3-HT*) in 1.5 ml distilled chloroform) to initiate the grafting process under nitrogen atmosphere. Solution containing the film was stirred (solution polymerization) at 0 ^oC for 24 h under nitrogen atmosphere. The homopolymer, poly(3-hexylthiophene) (*P3HT*) other than grafted *P3HT* was washed away after stirring in chloroform for 12 h. Finally, the films were washed with methanol (CH_3OH) and were dried at 65 ^oC overnight under reduced pressure in vacuum oven. Sulphonation (electrophilic substitution reaction) has been performed on the *P3HT* grafted *PVDF* and its *NH* films using chlorosulphonic (HSO_3Cl) acid at 65 ^oC for 2.5 h. The condition was optimized by altering the temperature and time so that mechanically stable polymer films were obtained after chemical modification for ready use in fuel cell application. The films were washed with deionized water after the sulphonation and were dried at 65 ^oC for 24 h under reduced pressure. Henceforth, we will term the etched, etched+graft and etched+graft+sulphonated specimens as *–e*, *–g*, and *–g–s*, respectively, both for pure PVDF and NH.

4.3 Results and discussion

4.3.1 Nanochannel fabrication:

The fabrication of nanochannel in poly(vinylidene fluoride) (PVDF) and its nanohybrid (NH), organically modified layered silicates dispersed in polymer matrix, has been carried out using high energy swift heavy ions (SHI) irradiation to create latent tract of nanometer dimension in the films followed by selective chemical etching to take out the amorphous zone exclusively. This is to mention that the passage of high energy ions through the polymer film melts the surrounding area (tens of nanometer diameters) due to ions–polymer matrix interactions and its rapid quenching converts them into amorphous track along with the generation of free radicals in the polymer chains as shown in **Scheme 4.1**.

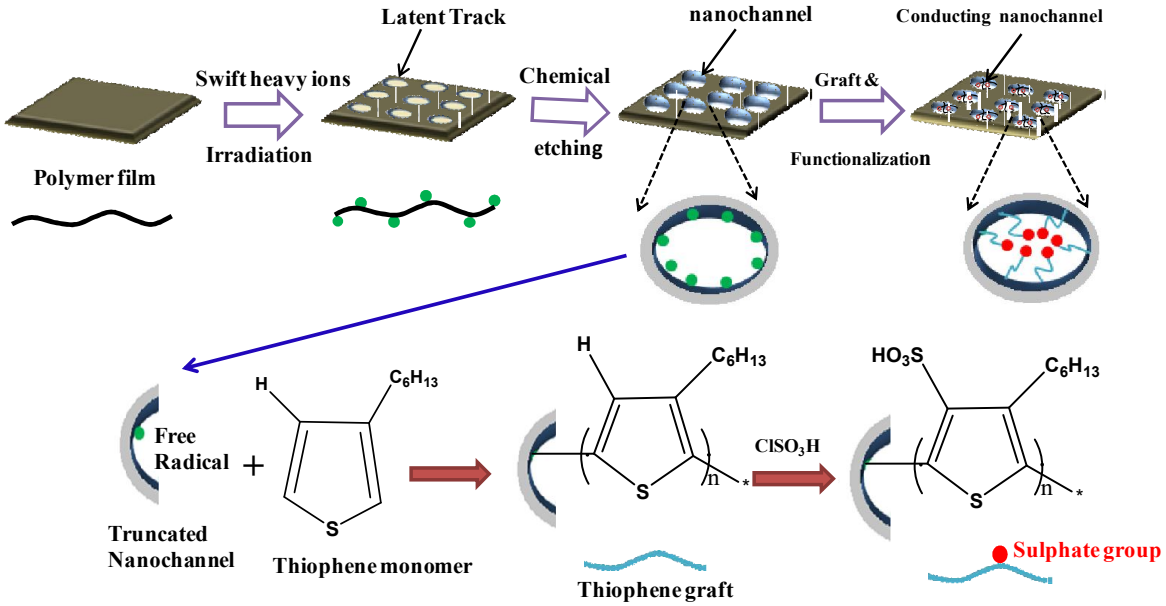

Scheme 4.1: Schematic representation of the swift heavy ions irradiation on polymer membrane, followed by selective chemical etching on irradiated membrane subsequent grafting within the nanochannels followed by sulphonation. Bottom column indicate the

grafting reaction within the nanochannel followed by its sulphonation to make the nanochannel conducting.

The dimension of track zones depends upon the linear energy transfer (LET) of swift heavy ions (120 MeV Ag^{+} with fluence 5×10^{7} ions/cm^{2}) [75].The dimension of the nanochannels was examined using AFM, showing black holes after etching of the irradiated specimen as indicated by the arrows in **Figure 4.1a** as opposed to the smooth surface before etching. The average dimensions of the nanochannels of PVDF and NH are 90±5 nm, 80±5 nm, respectively, with narrower distribution of channel size in nanohybrid as shown in the respective histogram. The formation of nanochannels is also confirmed through SEM images with similar dimension of holes and their distribution (**Figure 4.1b**). Interestingly, channel dimensions become regular and smaller in nanohybrid vis-à-vis irregular and bigger shape of holes in pure PVDF. Two dimensional rigid layered silicate platelets along with the needle like morphology (will be discussed later) in nanohybrid help restricted the amorphous track (which subsequently form the nanochannel) in almost circular shape against the asymmetrical track /channel in spherulite dominated pure PVDF. Further, the number density of nanochannel is quite high in nanohybrid as compared to pristine PVDF leading to the 10% of channel area in nanohybrid against 5% in pure PVDF [49]. The area of the nanochannels is measured from the number of channels multiplied by the average circular area of the channel. Moreover, the advantage of using Ag^{+} ion in this study is to create larger channel dimension (~80 - 90 nm) mainly because of its bigger size against the literature reported dimension of 60 and 45 nm using Si^{+}[106] or Li^{+} ions [19], respectively, in similar fluence of SHI. However, regulated and bigger dimension of nanochannels are

created in PVDF using nanoclay at moderate fluence which maintain the mechanical integrity of the film to be used in real application like fuel cell membrane.

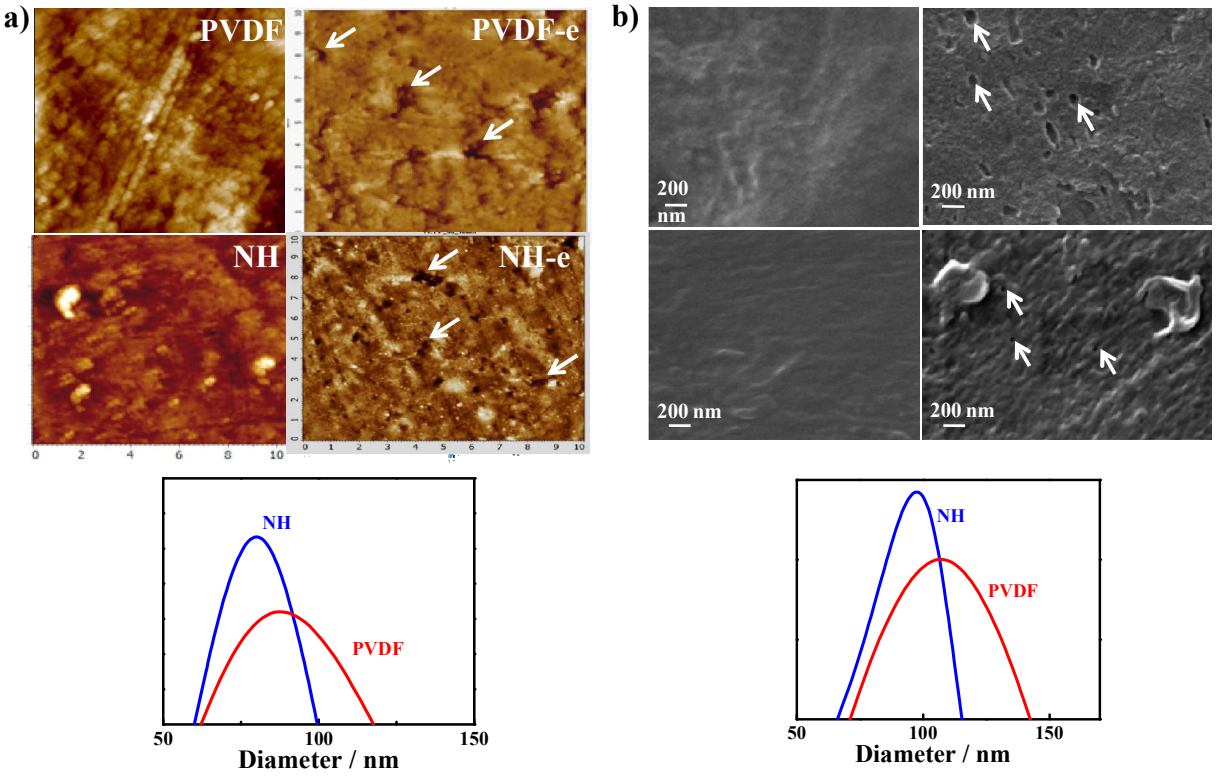

Figure 4.1: (a) AFM images of both PVDF and nanohybrid (NH) before and after radiation. The arrows indicate the location of channels. Histogram shows the distribution of channel dimension; **(b)** SEM images of pristine PVDF and NH, before and after irradiation and bottom histogram indicate distribution of channel dimension.

4.3.2 Grafting of PVDF and functionalization within the nanochannel:

Swift heavy ions irradiation bring certain chemical changes in polymer film like chain scission, double bond formation, bond breaking, formation of free radicals and other phenomena. Those free radicals are exclusively located in the amorphous latent track and

they remain at the periphery of the nanochannel after etching out of the amorphous zone. These free radicals at the edge of the nanochannels act as initiator and grafting with PVDF chains is designed using 3-HT monomer leading to the fill up of the nanochannel cylinder with conducting P3-HT graft followed by the sulphonation of P3-HT to make the nanochannel better conducting. The grafting and sulphonation is confirmed through H^1-NMR measurement from the appearance of the peaks at $\delta = 2.80$, 1.95 ppm for grafting of P3-HT on PVDF chains [182] and $\delta = 7.90$ ppm for graft sulphonation in P3-HT chain and $\delta = 8.2$, 7.7, 7.2 and 5.6 ppm peaks for the sulphonate proton [20, 40] in PVDF chain (direct sulphonation) as shown in **Figure 4.2a**. PVDF characteristic peaks appear at $\delta = 2.9$ and 2.3 ppm for head-to-tail and head-to-head, respectively [33,41]. The degrees of sulphonation are calculated from the integral peak areas and are found to be 25 and 30% for pure PVDF and nanohybrid, respectively. Higher degree of sulphonation is nanohybrid arise from its larger nanochannel volume which is subsequently filled with P3-HT graft. The grafting is also confirmed through FTIR measurement from the appearance of the peak positions at 1649 and 1730 cm^{-1} due to -C=C- and -C=S symmetrical stretching vibrations of thiophene aromatic ring attached with PVDF chain (**Figure 4.2b**). Moreover, symmetrical stretching frequency of aliphatic $–CH_3$ and $–CH_2–$ at 2926 and 2843 cm^{-1}, respectively, [183][184][185] as shown in **Figure 4.2c** along with 1415 cm^{-1} peak designated for CH_3- deformation vibration of the P3-HT group [186]**.** Stretching vibration band of sulphonate –OH group appears at 3400 cm^{-1} arises both in PVDF and its NH after sulphonation and its broadness suggested interactive system through hydrogen bonding (**Figure 4.2c**). The sulphonation in the main chain of PVDF is visualized through peak positions at 1047 [187] and 989 cm^{-1} due to SO_2 and SO_3^- vibration peak attached with

PVDF chain [188]. Further, the appearance of peaks at 836 and 1230 cm^{-1} for nanohybrid and sulphonated species indicate the presence of polar β– and γ–phase, respectively. This is worthy to mention that nanoclay nucleate β-phase in PVDF while grafting followed by sulphonation induce further polar β-phase in PVDF against the only α–phase peaks at 764 and 795 cm^{-1} observed in pure PVDF [18].

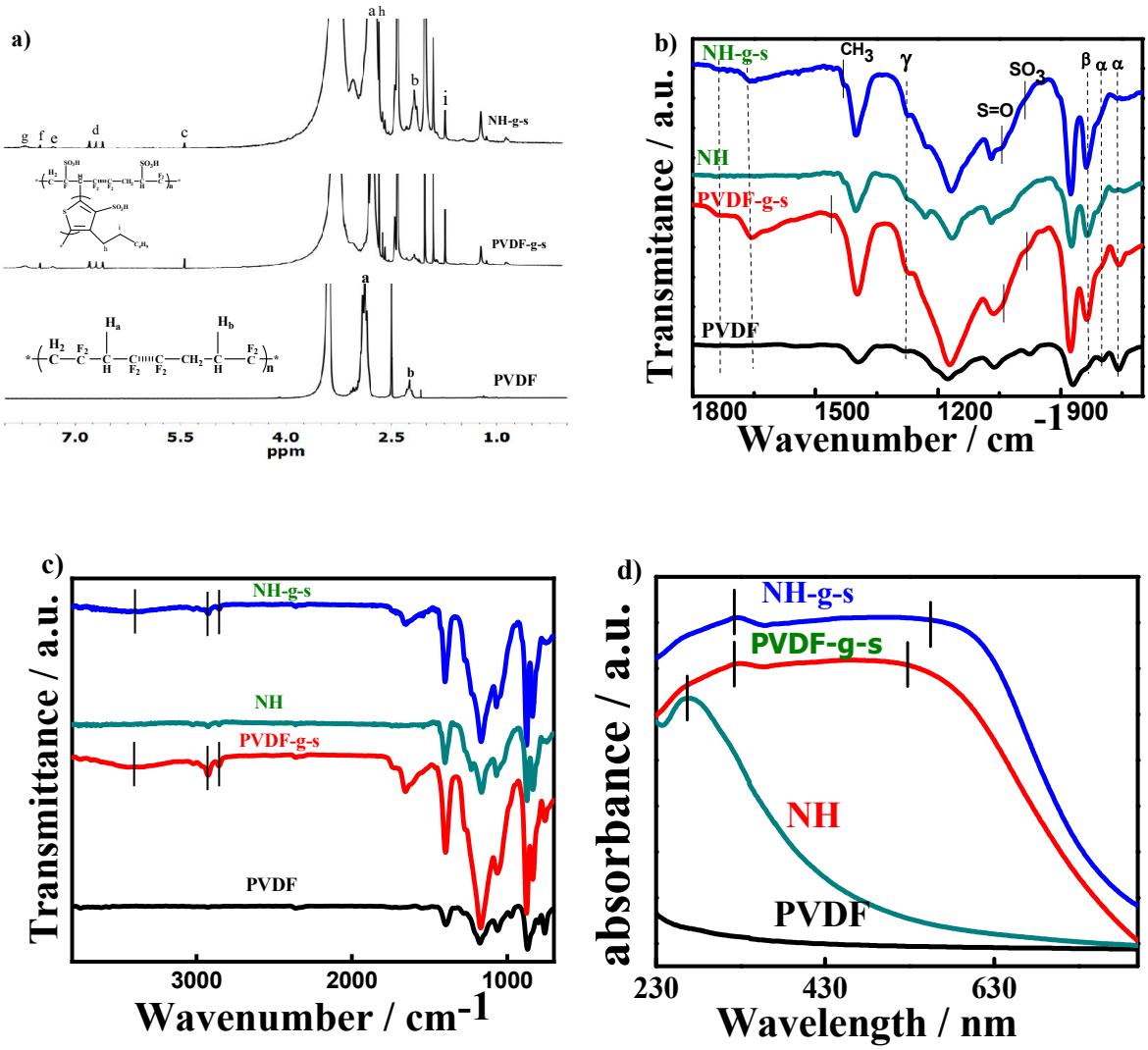

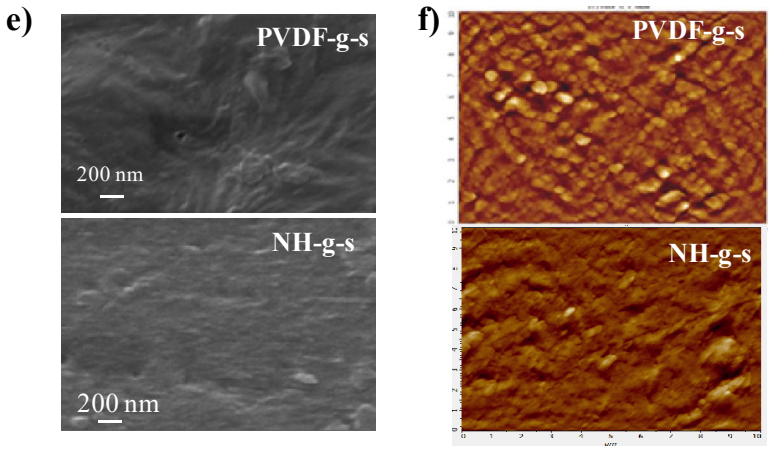

Figure 4.2: (a) ^{1}H-spectra of pristine PVDF, PVDF-g-s and NH-g-s measured using 500 MHz magnetic field NMR. Respective proton positions are indicated in the chemical structure (inset) and spectrum; **(b)** FTIR spectra of the pristine PVDF, PVDF-g-s, NH and NH-g-s indicating various peak assigned peak positions; **(c)** FTIR -spectra of PVDF, NH , PVDF-g-s, and NH-g-s functionalize membrane and indicate the stretching vibration frequency of hydrophilic group(-OH) through the vertical line.**(d)** UV-vis absorption spectra of PVDF, NH, PVDF-g-s and NH-g-s showing the peak position by vertical lines; and **(e)** SEM images of PVDF-g-s and NH-g-s showing filling up of channels after grafting; and **(f)** AFM image after grafting of indicate specimens showing filling up after grafting and functionalization.

UV-visible spectra of the specimens before and after grafting and functionalization are shown in **Figure 4.2d**. Pure PVDF does not show any absorption band while the nanohybrid exhibits a peak at 265 nm due to $\pi-\pi*$ transition arising from the C=C bond present in the organically modified nanoclay [89]. Further, a strong but broad band appears

at 513 nm observed in PVDF-g-s which is assigned to π–π* transition of the conjugated backbone of 3-HT graft along with absorption band of sulphonate group. Similar peak at 550 nm is observed in pure P3-HT while the significant blue shifts in PVDF-g-s occurs due to the confined conformation of grafted species within the constrained nanochannels [39], [84]. Interestingly, NH-g-s (functionalized nanohybrid) shows a wider band at 525 nm arises from the more number of nanochannels in nanohybrid. Further, another band at 325 nm became visible in both PVDF-g-s and NH-g-s, after grafting and sulphonation, due to n–π* transition in sulphonate group [90]. However, the spectroscopic measurements confirm the grafting of P3-HT and subsequent sulphonation within the nanochannels. Now, it is pertinent to show the effect of grafting and functionalization within the nanochannel following the process involved as shown in **Scheme 4.1**. Clear nanochannels are observed after etching out of the amorphous track caused by irradiation. SEM images of PVDF-g-s and NH-g-s clearly indicate no nanochannel in the membrane film resulting from the graft polymerization within the nanochannel (**Figure 4.2e**) which is further substantiated from the AFM micrographs of the above mentioned specimens about the filling up of the nanochannels (**Figure 4.2f**).

4.3.3 Structural modifications:

The effect of crystallinity and over all structural modification has been studied through wide angle X-ray diffraction. Semi crystalline structure of neat PVDF before irradiation show three distinct peaks at 2θ ~17.8^0, 18.4^0 and 20.06^0 corresponding to the crystalline planes of (100), (020) and (110) which indicate the presence of α-phase (*TGTḠ*) whose intensity decrease considerably after irradiation, grafting and functionalization (**Figure 4.3a**) primarily due to SHI induced amorphization [189]. On the other hand,

nanohybrid before irradiation exhibits peak at 20.30^{o} corresponding to (110)/(200) plane of piezoelectric β-phase (*TTTT*) while, contrary to PVDF, the intensity of the peak increases after grafting and functionalization leading to greater extent of β-phase [146], [189]. The quantitative analysis of phase fraction has been performed through deconvolution of XRD peaks showing considerable increase of β-phase in NH-g-s (72%) as opposed to meager presence of polar phase in PVDF (4%) in similar condition (**Figure 4.3b**). The β-phase fractions after grafting were 8 and 59% in PVDF-g and NH-g, respectively. This is to mention that PVDF does not possess any β-phase before irradiation while ~25% polar β-phase is observed in NH. Nanohybrid of PVDF copolymer with hexafluoropropylene (HFP) exhibits only 46% [49] of electro active β-phase under similar condition of SHI exposure followed by grafting with P3-HT and sulphonation against 72% in this study enhances significantly the electroactive phase in PVDF nanohybrid presumably due to better dispersion of nanoclay in PVDF in comparison to HFP copolymer. Spherulitic morphology of pristine PVDF vis-à-vis mesh-like morphology in nanohybrid under polarized optical microscope also consolidates the phase transformation in nanohybrid (**Figure 4.3c**). Grafting and subsequent functionalization changes the morphology towards needle like both in PVDF-g-s and NH-g-s which is similar to polar β-phase as discussed in XRD studies. However, grafting and sulphonation process induces the piezoelectric β-phase and its extent is significantly higher in nanohybrid as compared to pure PVDF. The origin of polar β-phase within the nanochannel is understood from the orientation of grafting in asymmetric manner which influence PVDF molecule to crystallize in β-phase. Further, greater crystallinity in NH-g-s helps improving the mechanical stability of the nanohybrid membrane.

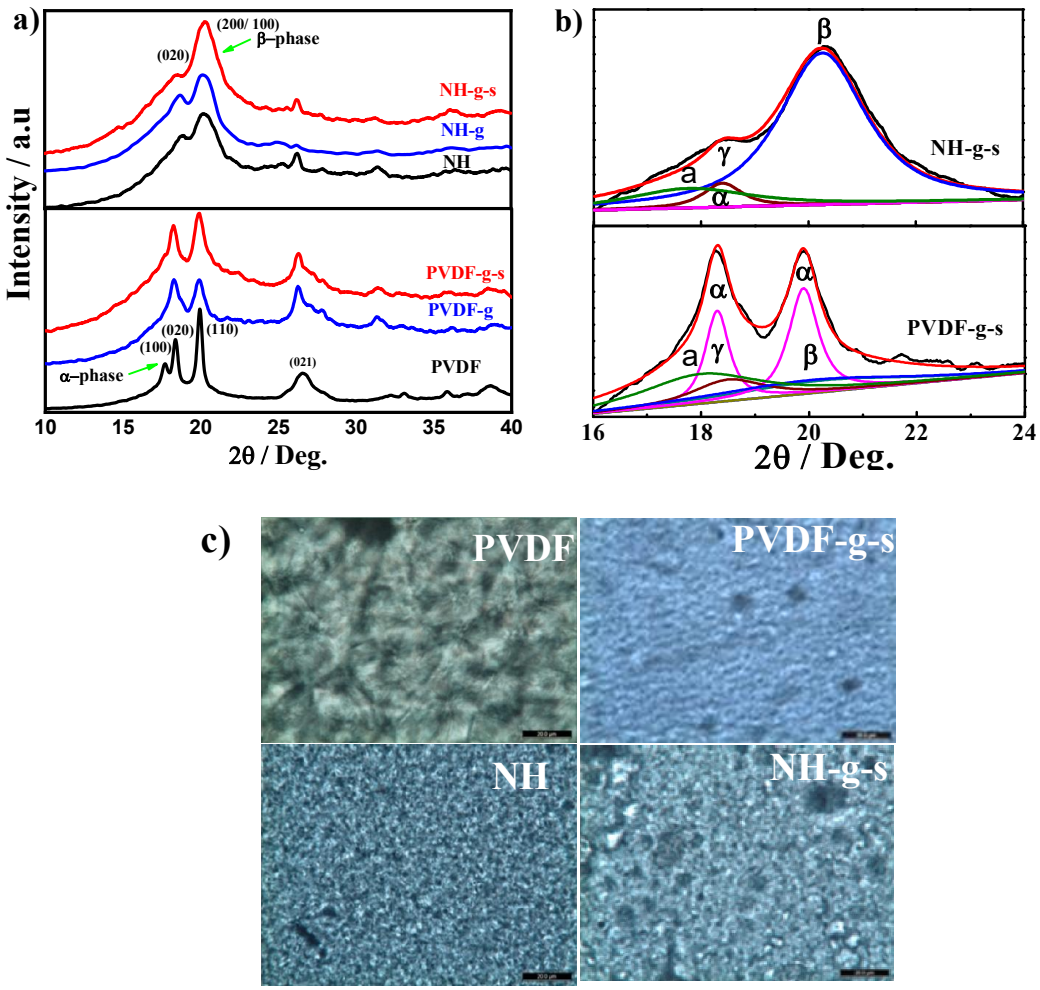

Figure 4.3 :(a) XRD patterns of indicate samples PVDF, PVDF-g, PVDF-g-s (lower column) and upper column show layered silicate dispersed specimen NH, NH-g, NH-g-s showing various crystalline planes; **(b)** Deconvulated XRD patterns of PVDF-g-s and NH-g-s showing different phases; and **(c)** Polarizing optical microscope image of PVDF, NH, PVDF-g-s and NH-g-s showing spherulite in PVDF and mesh-like morphology in NH while needle like morphology after grafting and functionalization

4.3.4 Effect of functionalization on thermal and electrical properties:

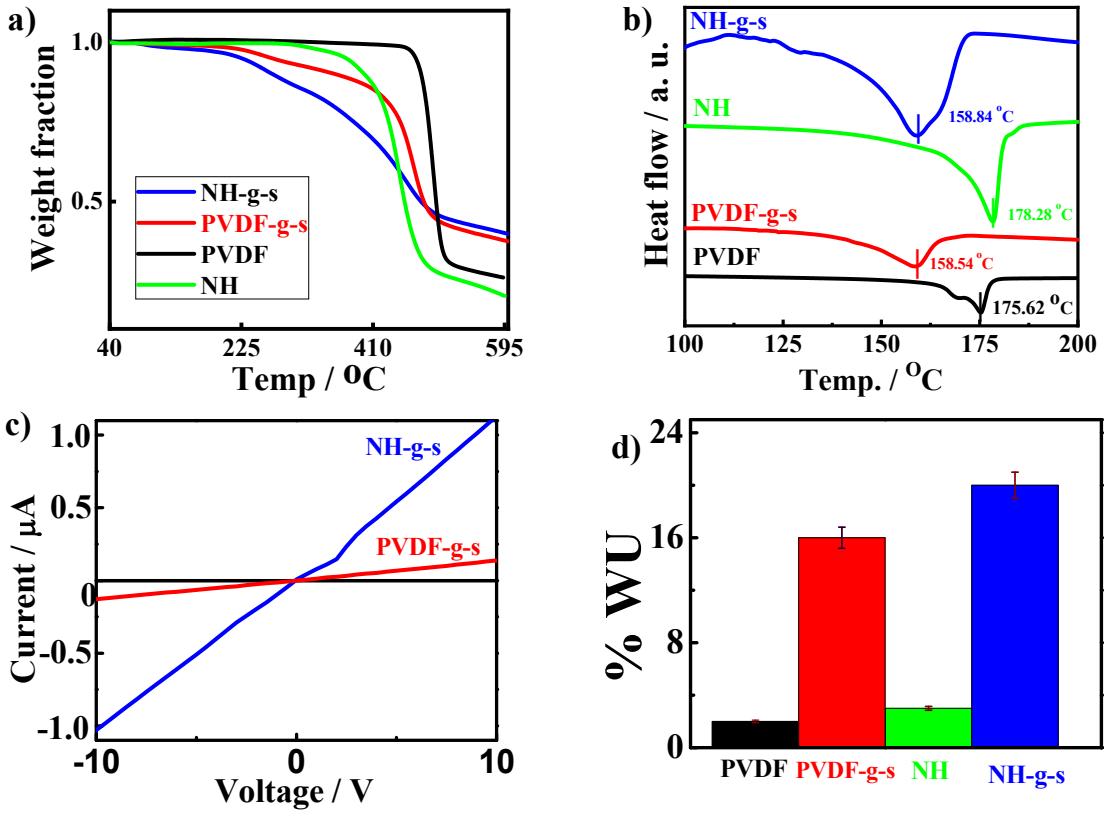

Figure 4.4: Thermal and electrical behavior of membranes **(a)** Thermograms of neat PVDF, NH and its grafted and sulphonated species (PVDF-g-s and NH-g-s); **(b)** DSC thermograms of PVDF/NH and their fictionalization membrane indicating the melting peak positions; **(c)** I-V measurement under DC electrical conductivity measurement; and **(d)** Water uptake values in percentage of the indicated membranes with error bars.

The thermal stability of neat PVDF, PVDF-g-s, NH and NH-g-s (graft and sulphonated specimens) are measured using a thermogravimetric analyzer (TGA) and the thermograms are presented in **Figure 4.4a**. Pure PVDF degrades at 471 °C corresponding to the 5 wt.% loss

showing a single sharp degradation step [190]. The degradation behavior remains similar for hybrid membrane but degradation temperature is shifted slightly to lower temperature as reported previously [191] while two steps degradation patterns are evident both for PVDF-g-s and NH-g-s. The first step of degradation display early degradation at 220 °C due to decomposition of sulphonate group (–SO_3H) attached with polymer chain and second step sharp degradation is due to the decomposition of main PVDF chains [98]. Greater degradation of functionalized nanohybrid is explained from the higher degree of sulphonation vis-à-vis PVDF. The melting behavior of PVDF, PVDF-g-s, NH and NH-g-s has been presented in **Figure 4.4b** showing decrease in melting temperature (T_m) by ~ 17 ^oC after grafting and sulphonation both for PVDF and its NH specimens presumably due to considerable amount of β-phase in functionalized membranes as discussed in XRD and morphology section in addition to the diluents effect in presence of P3-HT grafting on the PVDF chains [192], [193]. Slight higher melting temperature in NH as compared to PVDF is due to nucleation of γ-phase along with the piezoelectric β-phase in presence of 2-D Nanoclay [156]. DSC results support the FTIR studies of the formation of piezoelectric polar β- and partially polar γ-phases in nanohybrid while the extent of β-phase increases upon grafting and subsequent sulphonation as evident from the higher and sharp melting peaks of NH-g-s.

Current-voltage (I-V) characteristics curves of PVDF and its nanohybrid before and after grafting followed by sulphonation are shown in **Figure 4.4c**. As expected, pristine PVDF and NH exhibit very less current both at positive and negative bias indicating their insulating behavior when measurement perform while irradiated and functionalized membranes (PVDF-g-s and NH-g-s) display a systematic increase of current with the applied bias voltage and attain 100 and 1000 nA current at a bias voltage of 10 V for

PVDF-g-s and NH-g-s membranes, respectively. Greater degree of sulphonation arising from the comparatively large functionalized area (~10%) in nanohybrid is the reason behind the exhibition of significant higher current in NH-g-s as compared to functionalized PVDF under similar applied voltage and measure the electrical conductivity of functionalized membrane using the Van-der Pauw measurement (solid thin sample) [194] and found the conductivity of 4.4 $\times 10^{-6}$and 4.2×10^{-7} $S.cm^{-1}$ for NH-g-s and PVDF-g-s, respectively, due to linear chain (well ordered) configuration of conducting P3-HT polymer within confined nanochannels [195]. This alignment facilitates the transport of electrons while the grafting of styrene monomer, having coiled configuration inside the nanochannels, restrict the electron transport. Calculation of functionalized nanochannels area is done from the total surface area and area covered by the nanochannels considering the average diameter (area) multiplied by the number of nanochannels. Higher conductivity is also expected from the larger channel dimension with Ag^{+} exposed membrane (greater amount of grafting) as compared to relatively smaller channel dimension using Si^{+} or Li^{+} exposed membranes. However, more sulphonating groups attached with P3-HT as well as polymer chain is the driving force for better ions transport. Water uptake (WU) is an important criterion in determining the performance of proton exchange membrane as sufficient water is required as the mobile phase to assist proton conductivity and maintain the humidity of the membrane for fuel cell efficiency. Nanohybrid membrane (NH-g-s) shows higher water uptake (20%) as compared to functionalized PVDF membrane (15%) as shown in **Figure 4.4d** and the value of water uptake is similar to literature report [19]. This is to mention that pure PVDF and NH exhibit mere water uptake (less than 5%) arising from their hydrophobic character. However, grafting followed by sulphonation in

the nanochannel improve the hydrophilic character of the membrane suitable for proton conduction, essential criteria for any membrane to be used in fuel cell.

4.3.5 Proton conductivity and methanol permeability of the functionalized membrane:

Proton conductivity and methanol permeability are the two other important properties for a good proton exchange membrane besides all above properties mentioned of the developed membrane such as morphological criterion, thermal and mechanical stability, electrical properties and water uptake. Lower methanol permeability and higher proton conductivity are the major requirements of the polymer electrolyte membrane. To achieve better ion conduction, high anionic ionomer loading is generated through grafting followed by sulphonation in the nanochannels which are attached with the main chain chemically. The comparative study of proton conductivity is evaluated at a range of temperature of 30–80 ^{0}C and is presented in **Table 4.1 & 4.2** comparing the value of standard Nafion 117 membrane.

Table 4.1: Conductivities ($k^{m}\times10^{-2}$ S cm^{-1}) of indicated membranes (functionalized PVDF and nanohybrid) at different temperatures.

Temperature / **Membrane**	**30 ^{o}C**	**40 ^{o}C**	**50 ^{o}C**	**60 ^{o}C**	**70 ^{o}C**	**80 ^{o}C**
PVDF-g-s	4.21	4.69	5.31	6.08	7.06	7.84
NH-g-s	4.59	5.23	6.27	7.16	7.85	9.01

Table 4.2: Membrane conductivity (k^m), methanol permeability (P) at 30 ^oC, energy of activation (E_a) and power density values for different membranes measured at 30 ^oC using 30% methanol water mixture.

Membrane	k^m (10^{-2} S.cm^{-1})	P×10^{-7} cm^2.sec^{-1}	E_a (kJ mol^{-1})	Power Density mW/cm^2
PVDF-g-s	4.21	4.61	11.0	81.6
NH-g-s	4.59	4.49	11.3	92.0
Nafion117	9.66	13.1	6.5	63.3

Functionalized specimen (NH-g-s and PVDF-g-s) membranes shows proton conductivity of 4.59×10^{-2} and 4.21×10^{-2} S.cm^{-1}, respectively, showing considerable high proton conductivity in functionalized nanohybrid membrane as compared to functionalized PVDF especially in the higher temperature and achieve similar value of Nafion117 membrane (9.56×10^{-2} S.cm^{-1}) [8]. Higher proton conductivity in functionalized nanohybrid is primarily due to greater sulphonation in the grafted component within the nanochannels. However, both the functionalized membranes (PVDF-g-s and NH-g-s) show higher conductivity with increasing temperature exhibiting semiconducting nature of the membrane (**Figure 4.5a**). The activation energies (E_a) are calculated from the slope of the curves following the Arrhenius equation and are measured to be 11.0 and 11.3 kJ.mole^{-1} for PVDF-g-s and NH-g-s, respectively, vis-à-vis the much lower value of 6.5 kJ.mole^{-1} of standard Nafion117. Higher activation energy of the functionalized hybrid membrane indicate its greater stability at high temperature as compared to Nafion117 and clearly demonstrate the superior property of the developed membrane and overcome the shortcoming of the Nafion membrane specially at high temperature uses. This is to mention

that considerable lower conductivities of 1.22×10^{-2} and 2.55×10^{-2} S.cm^{-1} using Li^+ and Ag^+ ion as SHI with styrene are reported as expected from meager amount of grafting in smaller channels and non-conducting graft [19].

The methanol permeability across the membrane occurs in DMFC (direct methanol fuel cell) which increase at higher temperature when fuel pass one electrode (anode) to another electrode (cathode) and cause dropping of the open circuit voltage (OCV) resulting decrease of fuel cell efficiency. Methanol permeability along with proton conductivity, activation energy and power density values of the functionalized membranes are presented in **Table 4.2**. The methanol permeability values considerably reduce to 4.61×10^{-7} and 4.49×10^{-7} cm^{2}s^{-1} for functionalized PVDF and nanohybrid (PVDF-g-s and NH-g-s), respectively, from the higher value of Nafion117 (13.10×10^{-7} cm^{2}s^{-1}) (**Figure 4.5b**). The lower methanol permeability of functionalized nanohybrid membrane is due to greater barrier effect in presence of 2-D nanoclay platelet uniformly distributed in the polymer matrix [97]. The ratio of proton conductivity and methanol permeability describes the efficiency of the membrane in terms of selectivity parameter (SP) and the values of 1.02×10^5 and 0.91×10^5 S.cm^{-3}.s are calculated for NH-g-s and PVDF-g-s, respectively, indicating superior performance of functionalized membranes vis-à-vis Nafion117 membrane (SP = 0.73×10^5 S.cm^{-3}.s). Further, nanohybrid membrane exhibits better performance as compared to functionalized PVDF membrane in terms of lower methanol permeability, higher proton conduction and greater selectivity parameter along with improved water uptake. This is worthy to mention that all these superior properties in nanohybrid arise from its greater degree of sulphonation which leads to be a versatile membrane for fuel cell application. Moreover, the advantage of very less methanol

permeability enhance the fuel cell efficiency by reducing the voltage drop of fuel cell and in this work it is much lower against the literature reported membrane [49].

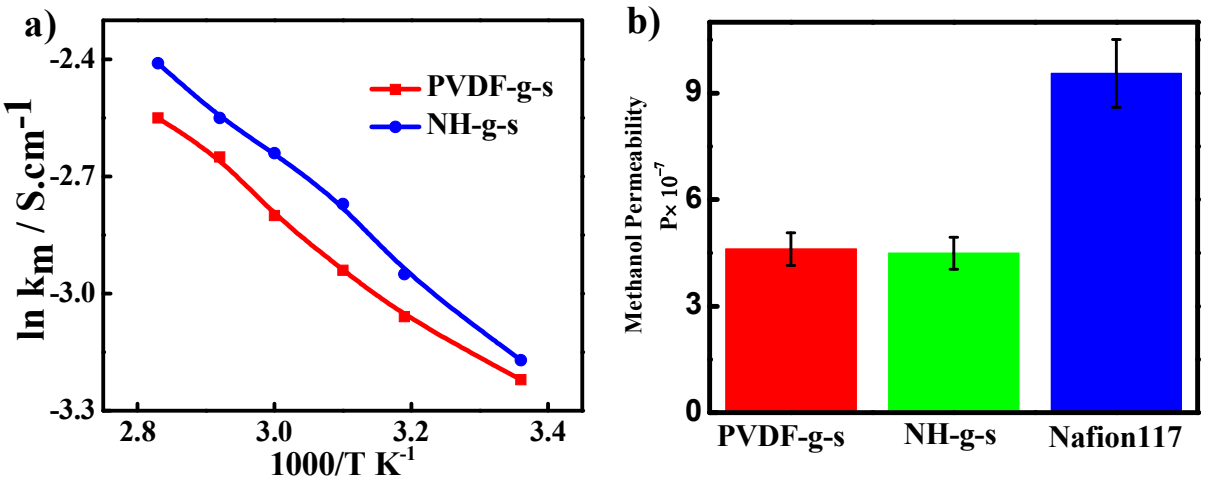

Figure 4.5: (a) Arrhenius plot (proton conductivity) k_m vs. 1/T for PVDF-g-s and NH-g-s; and **(b)** methanol permeability of indicated membranes comparing the standard Nafion117 values measured in similar condition.

4.3.6 Fuel cell efficiency in MEA stack:

Polarization (I-V characteristic) curve is used to measure the efficiency of fuel cell membrane in DMFC. Complex membrane electrode assembly (MEA) sequence is shown in **Figure 4.6a** and **Figure 4.6b** shows the fuel cell performance (polarization curves) of PVDF-g-s and NH-g-s membranes. Membrane electrode assembly (MEA) studies of functionalized nanohybrid and PVDF membrane show 0.753 and 0.713 V open circuit voltage (OCV), respectively, indicating better performance from nanohybrid membrane even as compared to the measured open circuit voltage of standard Nafion117 in similar condition (0.682 V OCV). A possible reason for higher value of OCV of nanohybrid membrane may lie on its

superior proton conductivity through the enhancement of grafting and sulphonation within the nanochannel which facilitate the cell performance. The power density of DMFC using NH-g-s shows very high value of 92.0 mW/cm^{2}at a current density of 252.60 mA/cm^2 against the value of 81.63 mW/cm^2 at a current density of 251.40 mA/cm^2 for functionalized PVDF (**Figure 4.6c**). This is to mention that Nafion117 exhibits 63.3 mW/cm^2 of power density at a current density of 219.21 mA/cm^2 in similar condition of measurement demonstrating superior fuel cell activity using functionalized nanohybrid as proton exchange membrane. The functionalized nanohybrid membrane exhibits higher OCV, power density, current density, water uptake and proton conductivity than that of functionalized PVDF and standard Nafion117 presumably due to greater grafting followed by sulphonation inside the nanochannel. However, Si^{+7} irradiated HFP-hybrid membrane followed by grafting (P3-HT) and sulphonation showed OCV of 0.68V, current density (140 mA / cm^2) and lower power density (45 mW / cm^2) [49]. Porous membrane using accelerator and subsequent grafting with styrene provide only 0.60 V OCV, current density 170 mA.cm^{-2}, power density 30 mW/cm^{-2} are much lower than the present work along with improved methanol permeability using PVDF nanohybrid membrane [19]. Further, 2-D nanoclay dispersed in polymer matrix convert it into piezoelectric β–phase whose content is auxiliary enhanced after sulphonation within the nanochannel and give rise to the possibility of smart membrane.

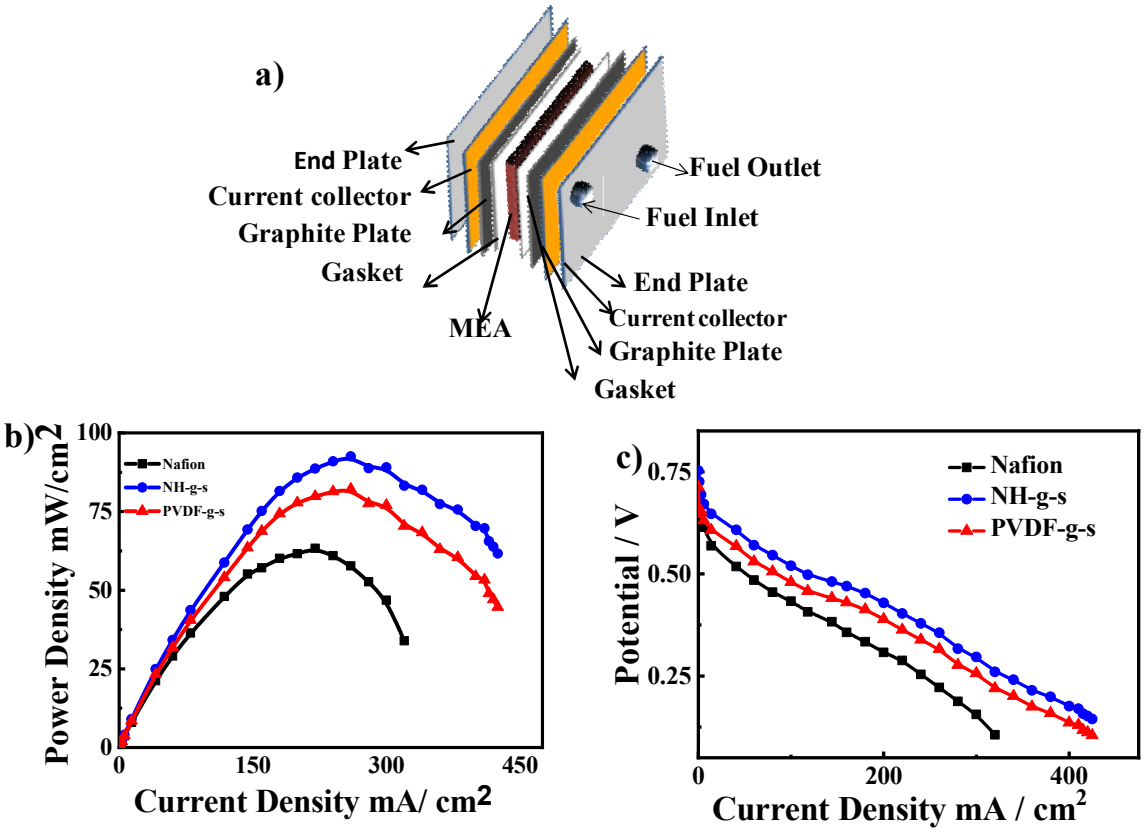

Figure 4.6: (a) A schematic illustration of the setup employed for the fuel cell efficiency test (complete cell stack with MEA); (b) comparison of polarization curves of indicated membranes; and (c) power density as a function of current density of indicated membranes comparing the values of standard Nafion measured in similar condition.

4.4 Conclusion

Hybrid proton exchange membrane has been developed by irradiating swift heavy ions using accelerator followed by functionalization for fuel cell application. Amorphous latent track of nanometer dimension caused by high energy swift heavy ion irradiation is selectively etched out chemically to create nanochannels of average diameter of 90 nm. Those

nanochannels are filled with conducting polymer using the free radicals generated during swift heavy ion passage at the periphery of the nanochannel walls followed by its sulphonation to make it better ion conducting. ^{1}H NMR and FTIR studies confirm the grafting and functionalization. 2-D layered silicates dispersed in polymer matrix convert it into piezoelectric β-phase (25%) whose content becomes significantly higher (72%) after functionalization of the membrane. Morphological investigation also supports the filling up of nanochannel and structural conversion (α- to β-phase). Thermal and mechanical stability of the membranes are measured through TGA and UTM, and are found appropriate for membrane applications. Water uptake of the hybrid membrane reached 20% and considerably high proton conductivity make the membrane suitable for fuel cell. Polarization curve of I-V characteristics also support the channel conductivity and proton conductivity of functionalized hybrid (NH-g-s) membrane is found to be 4.59×10^{-2} $S.cm^{-1}$. Methanol permeability, one of the important criteria for proton exchange membrane, is measured to be quite low (4.49×10^{-7} cm^2s^{-1}) as compared to pure polymer and standard Nafion117 (13.1×10^{-7} cm^2s^{-1}). Direct methanol fuel cell (DMFC) efficiency using the developed hybrid membrane has been measured and found excellent power density of 92.0 mW/cm^2 against the value of 63.6 mW/cm^2 of Nafion117 in similar condition. Relatively higher open circuit voltage (0.752 V) and current density (252.60 mA/cm^2) also indicate the superior fuel cell performance using functionalized hybrid membrane.